

Observation of suppressed viscosity in the normal state of ^3He due to superfluid fluctuations

Rakin N. Baten¹, Yefan Tian¹, Eric N. Smith¹, Erich Mueller¹, and Jeevak M. Parpia^{1,*}

¹Department of Physics, Cornell University, Ithaca, N.Y. 14853, USA
*jmp9@cornell.edu

ABSTRACT

We have observed a fluctuation-driven reduction in the viscosity of bulk ^3He in the normal state near the superfluid transition. While fluctuations are ubiquitous in two dimensional superconducting materials, in three dimensions fluctuations are thought to be limited to a very narrow region near the superfluid transition temperature, T_c , and thus uncommon. The observation of the fluctuation precursor is particularly relevant for measurements of transport to expose the topological nature of ^3He under strong confinement, where T_c is reduced. The normalized pressure dependence of the fluctuation contribution is found to be monotonic, and increases with pressure.

Introduction

In superconductors, fluctuations can be significant contributors to thermodynamic quantities (specific heat) and transport just above the superfluid transition temperature, T_c , especially in materials of reduced dimensionality, or with significant disorder. Superconducting fluctuations were first discussed by Ginzburg^{1,2}. However, bulk superfluid ^3He , a paradigm for exotic superconductors, is exceedingly clean and to date, fluctuations in ^3He have only been observed in the attenuation of zero sound (also known as collisionless sound)³⁻⁵. In the intervening time, both experimental and theoretical effort has been concentrated on zero sound⁶⁻⁹. However, Emery¹⁰ predicted that fluctuation contributions should be observable in the viscosity and spin diffusion (but not in thermal conductivity). Studies of transport in nano-confined ^3He are now feasible¹¹⁻¹⁶, where significant T_c suppression can be realized. Consequently, enhancement of fluctuations in the region between the suppressed T_c and the bulk T_c is expected. Strong confinement is expected to expose the topological nature of ^3He ¹⁷, while enabling the observation of anomalous effects such as mass and spin edge currents¹⁸⁻²⁰ and a thermal Hall contribution²¹. Thus, it is essential that an understanding of the contribution of fluctuations to transport be mapped out for the successful interpretation of quantitative transport measurements under strong confinement.

The Ginzburg criterion estimates the fluctuation contribution to dominate in a region $\delta T/T_c = (T_c/T_F)^4 \approx 10^{-12}$ (T_F is the Fermi temperature), much smaller than can be measured. However, Cooper pairs that condense below T_c can form above T_c with a finite lifetime (the lifetime is ∞ below T_c). Using dimensional arguments² the pair lifetime can be estimated to be $\tau_{GL} \approx \hbar/k_B(T - T_c)$. For ^3He at a temperature $\approx 1\%$ above T_c , $\tau_{GL} \approx 3 \times 10^{-7}$ sec, comparable to the quasiparticle scattering time. Thus “broken” Cooper pairs should contribute an additional scattering channel for diffusive processes and result in an increased viscosity.

Previous experiments that studied the viscosity^{22,23} had the resolution to observe contributions at the level of better than 1%. However, these experiments were carried out in a parameter space where the viscous mean free path was of order the confinement size ($\approx 135 \mu\text{m}$). Thus, the experiments were conducted in the slip dominated “Knudsen” regime which led to a modification of the effective viscosity away from the usual Fermi liquid behavior ($\eta(T) \propto T^{-2}$). These “size effects” were dominant at low pressure where the mean free path is longest. Experiments observed significant deviations from Fermi liquid behavior at all pressures. These observations were compounded by non-linearities in thermometric measurements. In consequence, departures from Fermi liquid behavior could not be solely attributed to fluctuations, or slip, or errors in thermometry, and fluctuation and size effect contributions could not be separated.

Results

The experimental results described here were obtained with a quartz fork²⁴ with dimensions much greater than the quasiparticle mean free path or viscous penetration depth ($\delta = (2\eta/\rho\omega)^{1/2}$, with η , ρ , the viscosity, density of the ^3He and ω the resonant frequency of the fork. The fork was driven on resonance and the temperature was measured with a diluted paramagnetic salt thermometer placed in the same ^3He volume proximate to the quartz fork. Additional details on fork operation and thermometry are provided in the methods section and the Supplemental information. The experiment was cooled by a nuclear

demagnetization stage²⁵ to mK temperatures. The pressure was maintained at a constant value using electronic feedback for each experimental temperature sweep.

The quartz fork's quality factor, Q ($Q = f_0/\Delta f$), where f_0 is the resonant frequency and Δf is the resonance linewidth) varies as $(\rho\eta)^{-1/2}$; the (Fermi liquid) viscosity varies as T^{-2} while the density is constant.²⁴ Thus, in the Fermi liquid regime, the fork's $Q \propto T$. The data obtained at several pressures from 0 bar to 27.8 bar are shown in Figure 1a,b). For each data set, we show the best linear fit line obtained as a dashed line passing through the origin. At all pressures, we observe a small increase in the Q (δQ) so that there is a perceptible departure from the Fermi liquid behavior just above T_c . At high pressure, the Q actually passes through a minimum in the normal state (see the inset to Figure 1c)). At low pressure, the excess Q is smaller, though it can be resolved. Upon entering in to the superfluid state, the Q sharply increases due to the rapid decrease in viscosity at T_c .^{22,26-28} The differences between high and low pressure results are highlighted in 1 c). The quality of the data is sufficient to illustrate the development of the excess Q (δQ) in Figure 1 d) with pressure. We note that Knudsen effects contribute strongly when the ratio of viscous penetration depth to measurement "size" is largest. This would occur at low pressure, where the superfluid transition temperature is lower and the coefficient of viscosity is largest^{22,29}, in contrast to what is seen in Figure 1.

Discussion

The quasiparticle lifetime should be decreased by the injection of "broken pairs" due to the finite lifetime of Cooper pairs above T_c . These pairs introduce a parallel scattering channel and should lead to a decreased viscosity (compared to the Fermi liquid value) as the temperature approaches T_c from above. The viscosity is proportional to the scattering time τ , ($\propto T^{-2}$). Emery¹⁰ writes the fluctuation contribution to the viscous scattering time τ as

$$\delta\tau/\tau = \Gamma \left(\frac{k_B T_F \tau}{\hbar} \right) (k_F \xi_{00})^{-3} \alpha [1 - (\theta^{1/2}/\alpha) \tan^{-1}(\alpha/\theta^{1/2})] \quad (1)$$

where the quantity $\delta\tau$ is the additional scattering time due to the broken pairs above T_c . Here θ is the reduced temperature ($\theta = \sqrt{T/T_c} - 1$), T_F is the Fermi temperature, Γ a numerical constant that depends on the pairing and the transport parameter (in this case viscosity, η). The unitless quantity $k_F \xi_{00}$ is the product of the Fermi wavevector and the pairing coherence length, and in bulk He-3 can be expressed as

$$(k_F \xi_{00})^2 = \frac{7\zeta(3)}{12\pi^2} \left(\frac{T_F}{T_c} \right)^2 \quad (2)$$

where $\zeta(3)$ is the Riemann Zeta function of order 3.

Since the $Q \propto \eta^{-1/2} \propto \tau^{-1/2}$, it follows that $\delta Q/Q = -1/2 \delta\tau/\tau$. We can rewrite $\tau(T) = \tau(T_c) \times (T_c/T)^2$ and $Q(T) = Q_c \times T/T_c$. Thus $(\delta\tau/\tau) = (\delta Q/Q_c) \times (T_c/T)$. This yields a modified version of Equation 1,

$$\begin{aligned} \frac{\delta Q(T)}{Q_c} &= \Gamma \left(\frac{k_B T_F \tau(T_c)}{\hbar} \right) \left(\frac{T_c}{T} \right) (k_F \xi_{00})^{-3} \alpha [1 - (\theta^{1/2}/\alpha) \tan^{-1}(\alpha/\theta^{1/2})] \\ &= C(P) \frac{\alpha}{1 + \theta} \left(1 - \frac{\theta^{1/2}}{\alpha} \tan^{-1} \frac{\alpha}{\theta^{1/2}} \right), \end{aligned} \quad (3)$$

where $C(P)$ is a pressure dependent constant and α is a fitting constant.

We plot the normalized excess Q ($\delta Q/Q_c$) against reduced temperature in Figure 2 a). We have used the experimental values of Q_c from the fits to the Fermi liquid behavior plotted in Figure 1 b). Without normalization, we find that the excess Q is pressure dependent, decreasing with pressure (See Figure 1 d)), and contributing ~5% to the value of Q at T_c at high pressure down to ~2% at the lowest pressure measured. After normalization (Figure 2 a)), we find that the pressure dependence persists. To compare the temperature dependent behavior of $\delta Q/Q_c$ to Eq 3, we plot the quantity $\delta Q/\delta Q_c$ against the reduced temperature in Figure 2 b). The near collapse of this normalized δQ is compared to the expected fit expressed in Eq. 3 (dashed line) in Figure 2 b). The fitting parameter α is found to be ≈ 0.44 , and is shown in Figure 3 (a).

The contributions to the prefactor in Eq. 3 are reasonably well known. After adjustment due to changes in the temperature scales in use at the time of the measurements (see Supplementary Note 1), we compare the values of the observed normalized excess $\delta Q/Q_c$, and the excess Q (δQ) as a function of the pressure to the calculated values based on Eq. 3. The agreement

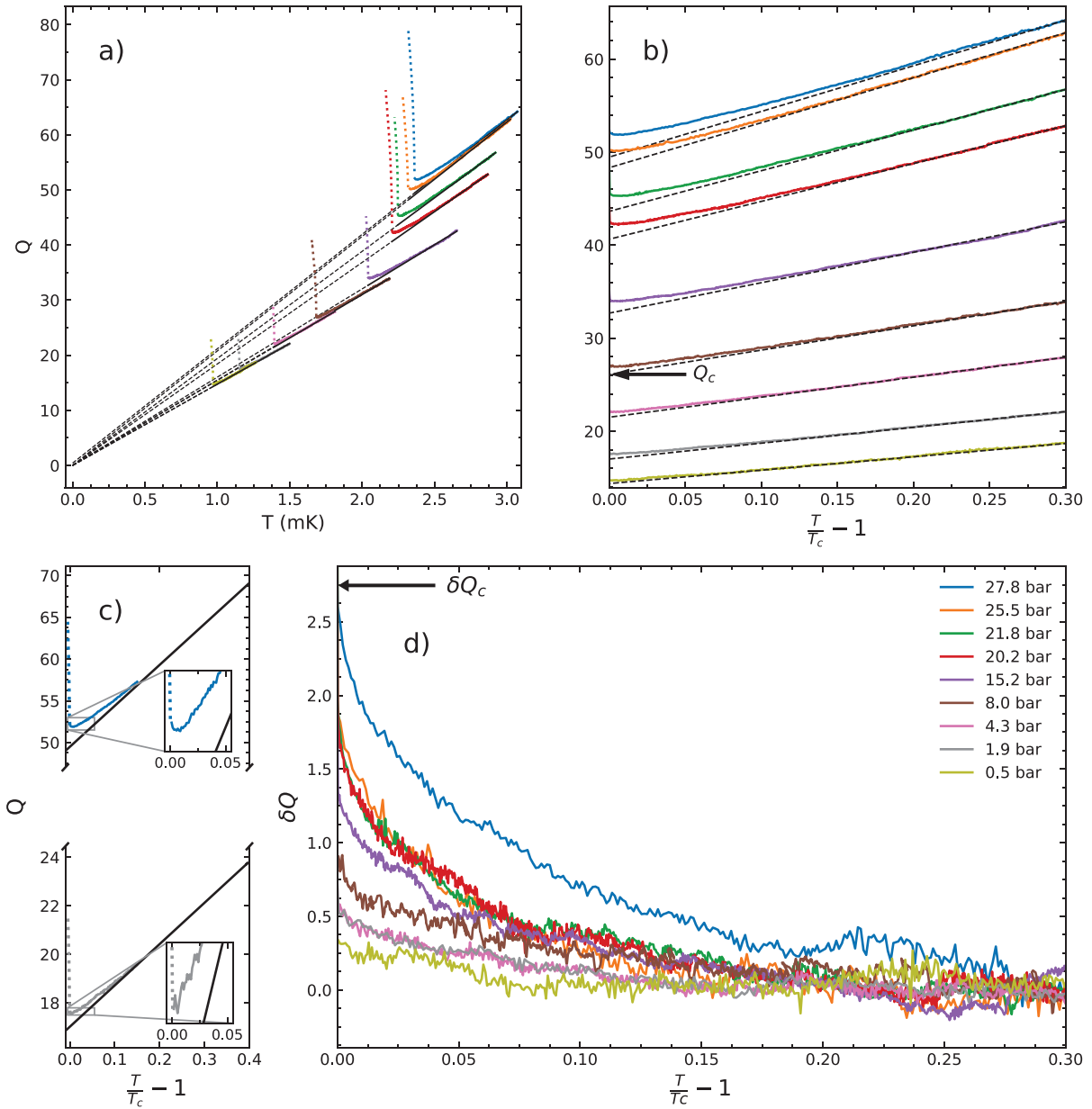


Figure 1. Quartz Fork Q vs Temperature a) The measured Q (after background subtraction) of the quartz fork at various pressures vs the temperature. The expected Fermi liquid behavior, $Q \propto \eta^{-1/2} \propto T$ is seen away from T_c as dashed lines. The superfluid transition is marked by an abrupt increase in the Q . Data in the superfluid is represented by a dotted line. b) Departure from the Fermi liquid behavior (linear slope) is seen at all pressures just above T_c . Also marked is the value of Q_c (value of Q at T_c without fluctuation contribution) for the 8 bar run. c) compares the Q vs $T/T_c - 1$ near T_c of the 27.8 bar and 1.9 bar runs. It is evident from the inset that the higher pressure run shows a minimum in the Q before T_c is attained, while the lower pressure data shows no minimum. d) we show the excess Q (δQ) after subtraction of the Fermi liquid behavior vs $T/T_c - 1$.

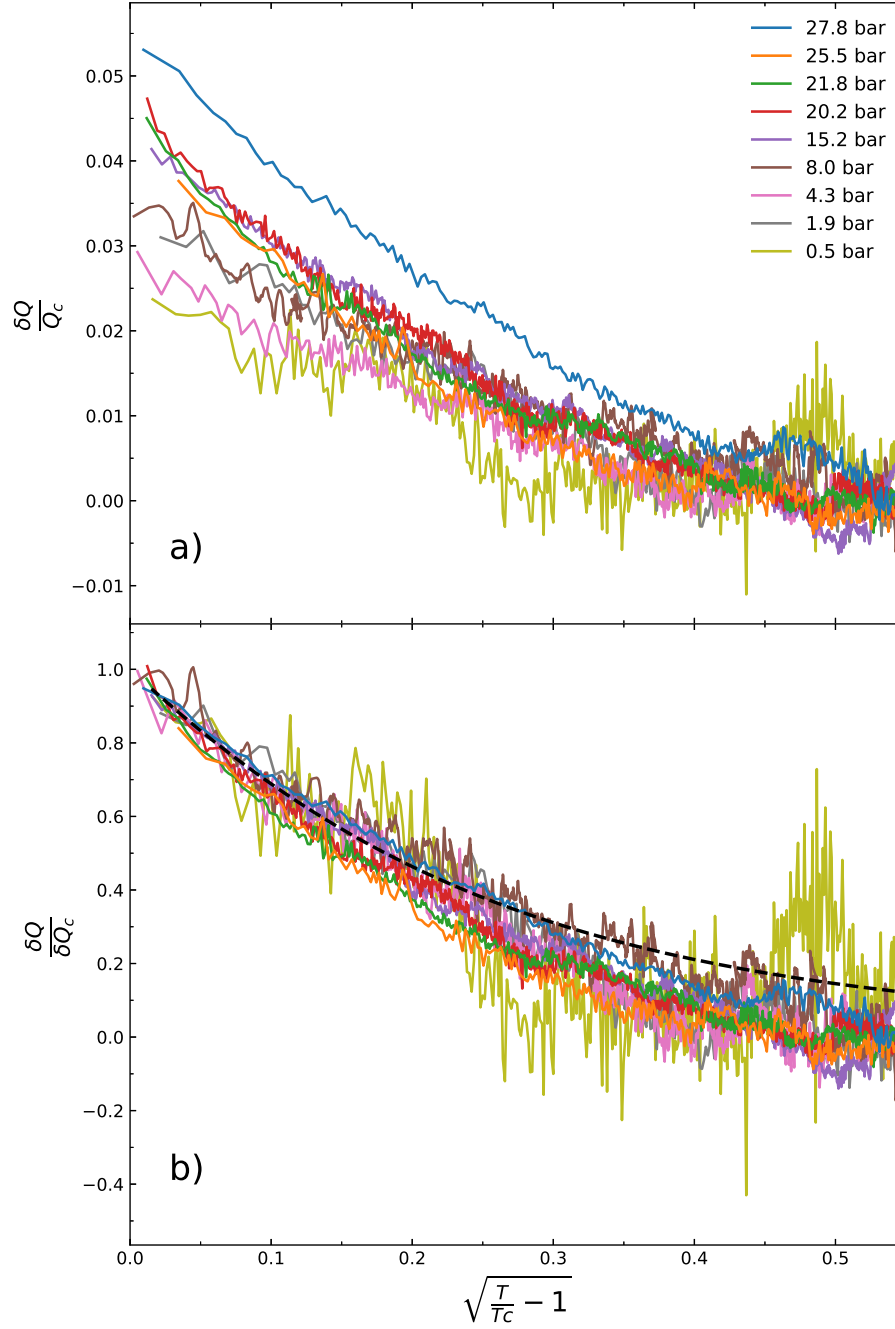


Figure 2. Normalized fluctuation Contribution vs reduced temperature a) The measured excess Q (δQ) after subtraction of the T linear Fermi liquid contribution (see Fig. 1 d)) of the quartz fork at various pressures, normalized to Q_c (see Fig 1b)) plotted against the square root of reduced temperature. This plot shows that the contribution to Q of the fluctuation component increases faster than the increase of Q_c with pressure. b) δQ normalized to the excess Q at T_c . The dashed line shows the expected temperature dependent fit to the fluctuation component of viscosity in Eq. 1 (see Ref [10]).

of the experimental results to the expectation is remarkably good. However, the value of Γ necessary to obtain a good fit (see the dashed line in Figure 3(b)) is of order 45, comparable to the maximum value quoted by Emery 10. We note that there is likely an error in the prefactor of order ~ 2 noted in Reference [9], which may account for the large value of Γ . Alternatively it is possible that a numerical correction factor to the value that we have used for τ is needed. (We used the viscous relaxation time (τ_η) and not the combination of τ_η , τ_{QP} noted in Ref [10]). In any event, the magnitudes of the fluctuation contribution to the viscosity are seen to be smaller than the values noted in References [3, 4].

The expression for the viscosity of the Fermi liquid $\eta = \frac{1}{5} n p_F \lambda_\eta$ (with n the particle density, p_F the Fermi momentum, and λ_η , the viscous mean free path), can be rewritten in terms of the relevant Landau parameters (F_1^s , F_2^s) in the form $\eta = \frac{1}{5} n \frac{m^*}{m} v_F^2 \tau_\eta = \frac{1}{5} n m (1 + \frac{F_1^s}{3}) (1 + \frac{F_2^s}{5}) v_F^2 \tau_\eta$. The values of F_2^s are poorly known⁹, as they are derived from the pressure dependence of the attenuation of transverse zero sound which a difficult to measure parameter³⁰. With planned improvements in signal recovery using low temperature amplifiers, the precision and noise of the excess Q should be greatly improved, and the pressure dependence and magnitude of this Landau parameter should be well-resolved.

Conclusion

We have observed that incipient pairing fluctuations contribute a small but significant portion of the scattering above T_c . This contribution is resolved at all pressures, and is comparable to that observed using the attenuation of collisionless (zero) sound. There are significant efforts underway to study transport processes (mass currents, viscosity and spin diffusion) in highly confined geometries where the suppression of T_c , and increased confinement may lead to the enhancement of fluctuations. The extreme purity of ^3He together with the low temperature of the superfluid transition result in the enhancement of fluctuations near T_c .

Methods

Fork operation: The quartz fork was operated in a phase locked loop and driven at a fixed drive voltage. The phase locked loop was set to drive the fork at a fixed frequency ± 5 Hz from the resonant frequency. When the frequency shift exceeded these bounds, the drive frequency was adjusted to bring the device on resonance again. The resonant frequency and Q were inferred from the complex response recorded by the lock in amplifier. In order to simplify this conversion, a significant background response of the non-resonant signal ("feedthrough") had to be measured and subtracted from the received signal. After subtraction, when the drive frequency was swept through resonance, the signal was seen to be Lorentzian, and was calibrated to yield the Q . Further details are provided in the Supplementary Note 2.

Thermometry: Thermometry was accomplished using a small pill (1.25 mm diameter, 1.25 mm high) of 30 μm powdered Lanthanum diluted Cerous Magnesium Nitrate (LCMN), packed to 50% density. The pill and monitoring coil were located in a niobium shielding can. The coil structure consisted of an astatically wound secondary and primary coil. The primary coil was driven at constant voltage through a 10 k Ω resistor by a signal generator at fixed frequency (23Hz). The secondary coil was coupled to the input of a SQUID. The secondary loop had an additional mutual inductor to allow cancellation of the induced signal in the loop. The input of this mutual inductor was driven by the same signal generator as the primary. The drive amplitude and phase of this cancellation signal was stepped by discrete amounts to cancel out most of the current in the secondary loop. The drive applied to the mutual inductor and the magnitude of the received signal were proportional to the susceptibility of the LCMN. These were calibrated against a melting curve thermometer and against the superfluid transition temperatures at various pressures. The thermometer had a resolution of better than 5 μK .

References

1. Ginzburg, V. & Landau, L. Phenomenological theory. *J. Exp. Theor. Phys. USSR* **20**, 17 (1950).
2. Larkin, A. I. & Varlamov, A. A. *Fluctuation Phenomena in Superconductors* (Springer Berlin Heidelberg, Berlin, Heidelberg, 2008).
3. Paulson, D. N. & Wheatley, J. C. Incipient superfluidity in liquid ^3He above the superfluid transition temperature. *Phys. Rev. Lett.* **41**, 561–564, DOI: [10.1103/PhysRevLett.41.561](https://doi.org/10.1103/PhysRevLett.41.561) (1978).
4. Samalam, V. K. & Serene, J. W. Zero-sound attenuation from order-parameter fluctuations in liquid ^3He . *Phys. Rev. Lett.* **41**, 497–500 (1978).
5. McClintock, P. V. E. Incipient superfluidity in normal liquid ^3He . *Nature* **275**, 585–586, DOI: [10.1038/275585a0](https://doi.org/10.1038/275585a0) (1978).

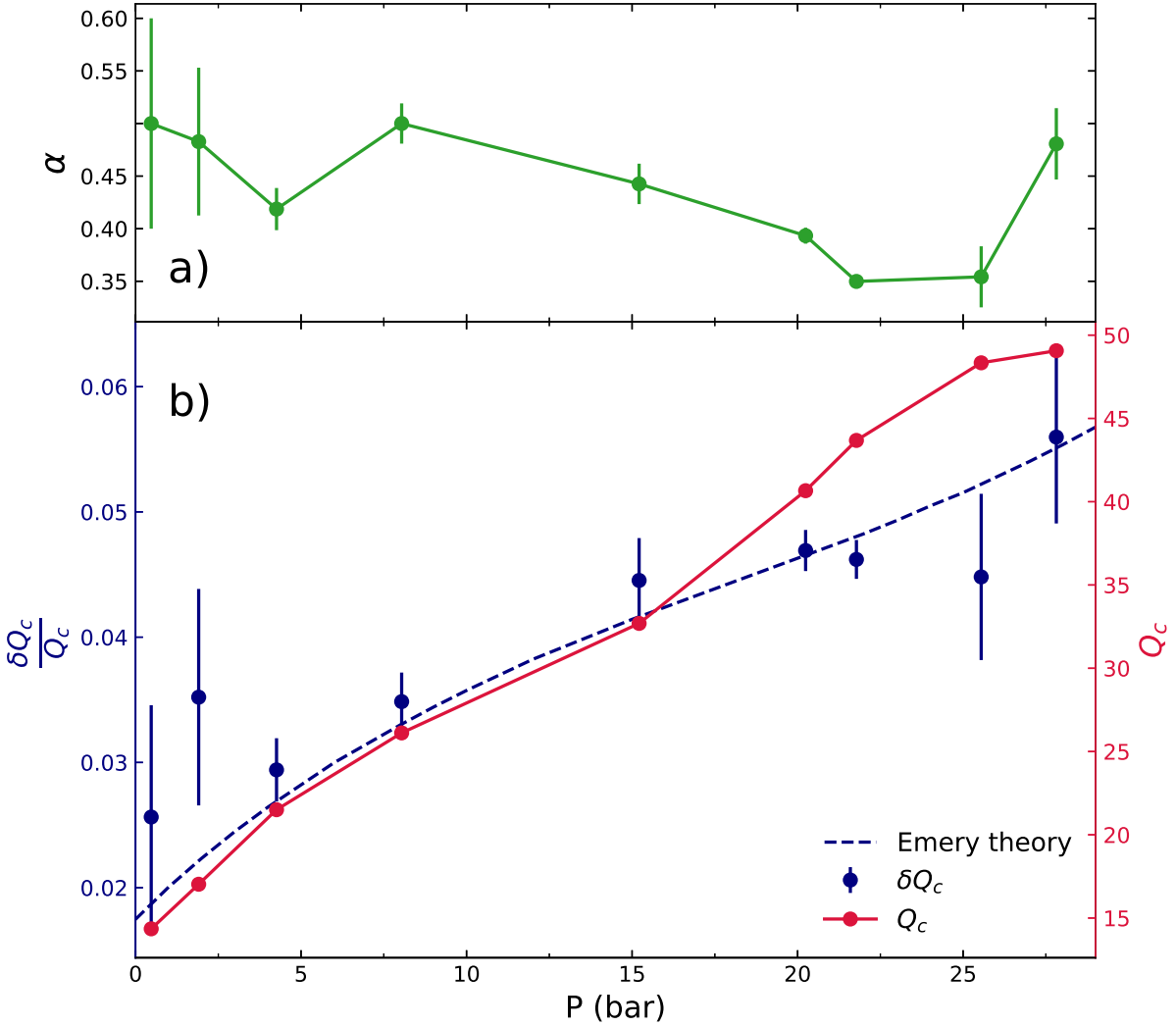


Figure 3. Comparison of measured and calculated parameters a) the values of α obtained to yield the fit shown in Figure 2(b). b) The measured excess Q at T_c (δQ_c , normalized to the value of the extrapolated Q at T_c (Q_c) based on the expectation of a Fermi-liquid viscosity as a function of pressure (blue points). Additionally, the measured values of Q_c based on the linear fits shown in Figure 1 is also plotted (red points). The dashed line shows the expected temperature dependent fit to the fluctuation component of viscosity in Eq. 1 (see Ref [10]) based on previously measured values of ηT^2 (Ref [29]), v_F , n and m^*/m (Ref [31]).

6. Lee, Y. C. *et al.* High frequency acoustic measurements in liquid ^3He near the transition temperature. *J. Low Temp. Phys.* **103**, 265–272 (1996).
7. Granroth, G. E., Masuhara, N., Ihas, G. G. & Meisel, M. W. Broadband frequency study of the zero sound attenuation near the quantum limit in normal liquid ^3He close to the superfluid transition. *J. Low Temp. Phys.* **113**, 543–548 (1998).
8. Pal, A. & Bhattacharyya, P. Fluctuation contribution to the velocity and damping of sound in liquid ^3He above the superfluid transition temperature. *J. Low Temp. Phys.* **37**, 379–387 (1979).
9. Lin, W.-T. & Sauls, J. A. Effects of incipient pairing on nonequilibrium quasiparticle transport in Fermi liquids. *Prog. Theor. Exp. Phys.* **2022**, DOI: [10.1093/ptep/ptac027](https://academic.oup.com/ptep/article-pdf/2022/3/033102/43061384/ptac027.pdf) (2022). 033102, <https://academic.oup.com/ptep/article-pdf/2022/3/033102/43061384/ptac027.pdf>.
10. Emery, V. Fluctuations above the superfluid transition in liquid ^3He . *J. Low Temp. Phys.* **22**, 467, DOI: [10.1007/BF00654719](https://doi.org/10.1007/BF00654719) (1978).
11. Levitin, L. V. *et al.* Phase Diagram of the Topological Superfluid ^3He Confined in a Nanoscale Slab Geometry. *Science* **340**, 841–844, DOI: [10.1126/science.1233621](https://doi.org/10.1126/science.1233621) (2013).
12. Levitin, L. *et al.* Surface-Induced Order Parameter Distortion in Superfluid $^3\text{He-B}$ Measured by Nonlinear NMR. *Phys. Rev. Lett.* **111**, 235304 (2013).
13. Zhelev, N. *et al.* The A-B transition in superfluid helium-3 under confinement in a thin slab geometry. *Nat. Commun.* **8**, 15963 (2017).
14. Heikkinen, P. J. *et al.* Fragility of surface states in topological superfluid ^3He . *Nat. Commun.* **12**, 1574, DOI: [10.1038/s41467-021-21831-y](https://doi.org/10.1038/s41467-021-21831-y) (2021).
15. Lotnyk, D. *et al.* Thermal transport of helium-3 in a strongly confining channel. *Nat. Commun.* **11**, 4843 (2020).
16. Lotnyk, D. *et al.* Path-dependent supercooling of the ^3He superfluid $a - b$ transition. *Phys. Rev. Lett.* **126**, 215301, DOI: [10.1103/PhysRevLett.126.215301](https://doi.org/10.1103/PhysRevLett.126.215301) (2021).
17. Mizushima, T., Tsutsumi, Y., Sato, M. & Machida, K. Symmetry protected topological superfluid $^3\text{He-b}$. *J. Physics: Condens. Matter* **27**, 113203, DOI: [10.1088/0953-8984/27/11/113203](https://doi.org/10.1088/0953-8984/27/11/113203) (2015).
18. Sauls, J. A. Surface states, edge currents, and the angular momentum of chiral p -wave superfluids. *Phys. Rev. B* **84**, 214509, DOI: [10.1103/PhysRevB.84.214509](https://doi.org/10.1103/PhysRevB.84.214509) (2011).
19. Wu, H. & Sauls, J. A. Majorana excitations, spin and mass currents on the surface of topological superfluid $^3\text{He} - \text{B}$. *Phys. Rev. B* **88**, 184506, DOI: [10.1103/PhysRevB.88.184506](https://doi.org/10.1103/PhysRevB.88.184506) (2013).
20. Wu, H. & Sauls, J. A. Majorana excitations, spin and mass currents on the surface of topological superfluid $^3\text{He-b}$. *Phys. Rev. B* **88**, 184506, DOI: [10.1103/PhysRevB.88.184506](https://doi.org/10.1103/PhysRevB.88.184506) (2013).
21. Sharma, P., Vorontsov, A. B. & Sauls, J. A. Disorder induced anomalous thermal hall effect in chiral phases of superfluid ^3He , DOI: [10.48550/ARXIV.2209.04004](https://arxiv.org/abs/2209.04004) (2022).
22. Parpia, J. M., Sandiford, D. J., Berthold, J. E. & Reppy, J. D. Viscosity of liquid $^3\text{He-b}$ near the superfluid transition. *Phys. Rev. Lett.* **40**, 565–568, DOI: [10.1103/PhysRevLett.40.565](https://doi.org/10.1103/PhysRevLett.40.565) (1978).
23. Tian, Y., Smith, E., Reppy, J. & Parpia, J. Anomalous inferred viscosity and normal density in a torsion pendulum. *J. Low Temp. Phys.* **205**, 226–234, DOI: [10.1007/s10909-021-02619-2](https://doi.org/10.1007/s10909-021-02619-2) (2021).
24. Blaauwgeers, R. *et al.* Quartz tuning fork: Thermometer, pressure- and viscometer for helium liquids. *J. Low Temp. Phys.* **146**, 537–562, DOI: [10.1007/s10909-006-9279-4](https://doi.org/10.1007/s10909-006-9279-4) (2007).
25. Parpia, J. *et al.* Optimization procedure for the cooling of liquid ^3He by adiabatic demagnetization of praseodymium nickel. *Rev. Sci. Instruments* **56**, 437 – 443 (1985).
26. Alvesalo, T. A., Anufriyev, Y. D., Collan, H. K., Lounasmaa, O. V. & Wennerström, P. Evidence for superfluidity in the newly found phases of ^3He . *Phys. Rev. Lett.* **30**, 962–965, DOI: [10.1103/PhysRevLett.30.962](https://doi.org/10.1103/PhysRevLett.30.962) (1973).

27. Pethick, C. J., Smith, H. & Bhattacharyya, P. Viscosity and thermal conductivity of superfluid ^3He : Low-temperature limit. *Phys. Rev. Lett.* **34**, 643–646, DOI: [10.1103/PhysRevLett.34.643](https://doi.org/10.1103/PhysRevLett.34.643) (1975).
28. Bhattacharyya, P., Pethick, C. J. & Smith, H. Transport and relaxation processes in superfluid ^3He close to the transition temperature. *Phys. Rev. B* **15**, 3367–3383, DOI: [10.1103/PhysRevB.15.3367](https://doi.org/10.1103/PhysRevB.15.3367) (1977).
29. Parpia, J. *The Viscosity of Normal and Superfluid ^3He* . Ph.D. thesis, Cornell University (1979).
30. Roach, P. R. & Ketterson, J. B. Observation of transverse zero sound in normal ^3He . *Phys. Rev. Lett.* **36**, 736–740, DOI: [10.1103/PhysRevLett.36.736](https://doi.org/10.1103/PhysRevLett.36.736) (1976).
31. Greywall, D. ^3He specific heat and thermometry at millikelvin temperatures. *Phys. Rev. B* **33**, 7520 – 7538 (1986).

Acknowledgements (not compulsory)

This work was supported by the National Science Foundation, under DMR-2002692 (Parpia), and PHY-2110250 (Mueller).

Author contributions statement

Experimental work was principally carried out by Y.T. and R.B. with further support from E.N.S. and J.M.P. Analysis and the presentation of figures was carried out by R.B. and Y.T. E.M significantly contributed to the analysis and the writing of the manuscript, J.M.P. supervised the work and J.M.P., and E.M. had leading roles in formulating the research and writing this paper. R.B and Y.T contributed equally to the publication of this result. All authors contributed to revisions to the paper.

Additional information

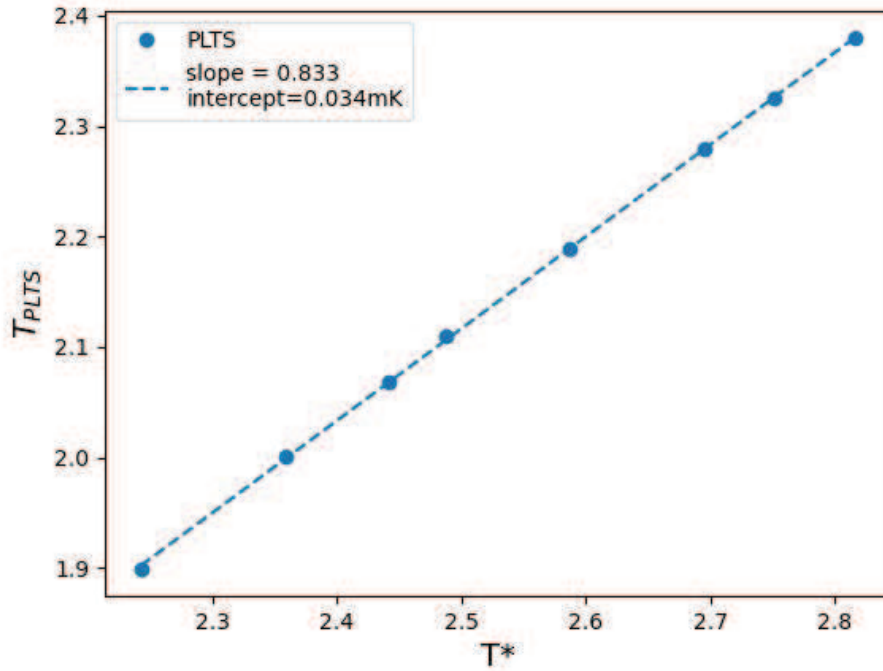
To include, in this order: **Accession codes** (where applicable); **Competing interests** (mandatory statement).

The corresponding author is responsible for submitting a [competing interests statement](#) on behalf of all authors of the paper. This statement must be included in the submitted article file.

Pressure [bar]	0	3	6	9	12	15	18	21	24	27	30
$\tau_\eta T^2$ [μsmK^2]	0.985	0.861	0.776	0.712	0.660	0.616	0.597	0.550	0.529	0.515	0.508
$\tau_\eta(T_c)$ [μs]	1.19	0.533	0.328	0.234	0.182	0.149	0.127	0.111	0.100	0.0933	0.0887
T_c [mK]	0.9097	1.271	1.539	1.743	1.903	2.033	2.139	2.226	2.296	2.351	2.392
T_F [K]	1.77	1.66	1.56	1.49	1.42	1.36	1.31	1.26	1.22	1.17	1.13
V_m [cm^3]	36.84	33.95	32.03	30.71	29.71	28.89	28.18	27.55	27.01	26.56	26.17
m^*/m	2.80	3.16	3.48	3.77	4.03	4.28	4.53	4.77	5.02	5.26	5.50
v_F [m/s]	59.83	54.53	50.38	47.11	44.49	42.32	40.44	38.74	37.15	35.65	34.24

Table 1. Table 1: Fermi liquid parameters Listed is a table of various quantities to estimate the fluctuation contribution in Equation 3, Main article

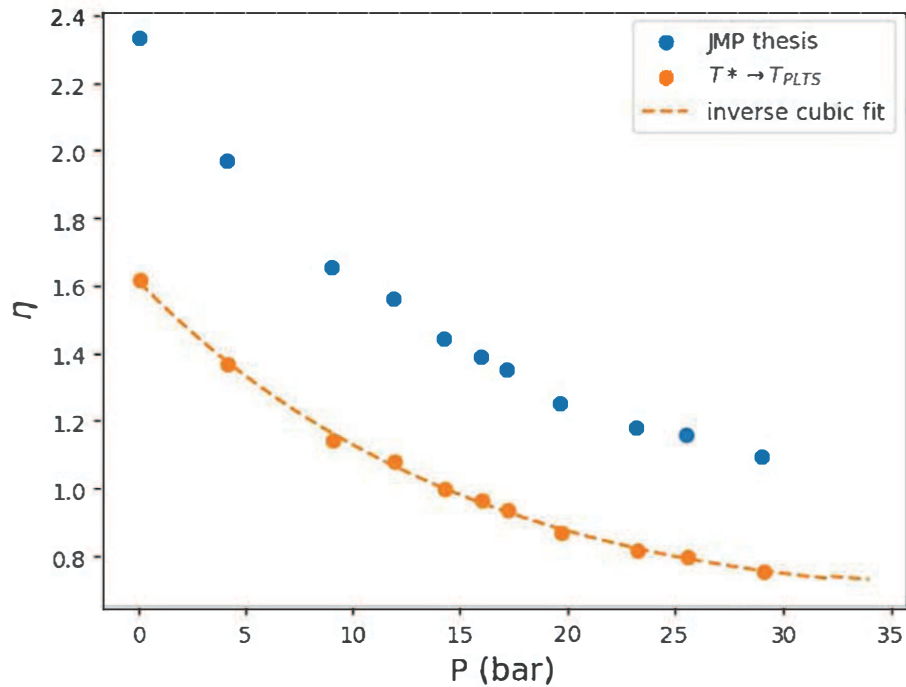
Supplementary Note 1: Calculation of $\tau_\eta T^2$ and other parameters



Supplementary Figure 1. Conversion from T^* to T_{PLTS} . Values of T_c^* ^{S1} plotted against values of T_c on the PLTS scale^{S2,S3}.

To arrive at an estimate for the magnitude of the fluctuation contribution to the Q , we need to determine various pressure dependent quantities of liquid ^3He . We start with the determination of $\tau_\eta T^2$, the quasiparticle scattering time associated with the viscosity. The Fermi liquid viscosity was studied by Parpia and co-workers^{S1}. The temperature scale used in this work needs to be converted to the PLTS scale^{S2}. We plot the values of T_c^* against the values of T_c in the PLTS scale^{S3} in Supplementary Figure 1. The conversion requires a linear scaling with a small offset, yielding $T_{PLTS} = 0.833T^* + 0.034$. The pressure dependent viscosity coefficients ηT^2 [poise-mK²] listed in Ref[1] are then converted to their values with the PLTS scale.

The viscosity coefficient [ηT^2 (η in poise, T in mK following the PLTS scale)] can be calculated from the relation, $(\eta T^2)^{-1} = \Sigma A_i P^i$ with $A_0 = 6.18470415\text{e-}01$, $A_1 = 2.49235869\text{e-}02$, $A_2 = 2.33758602\text{e-}04$, $A_3 = -9.37151796\text{e-}06$ and where P is the pressure in bar.



Supplementary Figure 2. ηT^2 vs Pressure. Values of the viscosity coefficient^{S1} before conversion (blue) and after conversion to the PLTS scale (gold). The dashed line is the cubic fit discussed in the text.

References

- [S1] Parpia, J. M., Sandiford, D. J., Berthold, J. E. & Reppy, J. D. Viscosity of normal and superfluid helium three. *J. Phys. Colloques C6* **39**, C6-35–C6-36 (1978). URL <https://doi.org/10.1051/jphyscol:1978617>.
- [S2] Rusby, R. *et al.* Realization of the 3 He Melting Pressure Scale, PLTS-2000. *J. Low Temp. Phys.* **149**, 156–175 (2007).
- [S3] Tian, Y., Smith, E. N. & Parpia, J. Conversion between 3He melting curve scales below 100 mk. *Journal of Low Temperature Physics* **184**, 1573–7357 (2022). URL <https://doi.org/10.1007/s10909-022-02721-z>.